Effect of Magnetic Field on the Microstructure and Macrosegregation in Directionally Solidified Pb-Sn Alloys

S.N. TEWARI, RAJESH SHAH, and HUI SONG

An investigation into the influence of a transverse magnetic field (0.45 T) on the mushy zone morphology and macrosegregation in directionally solidified hypoeutectic Pb-Sn alloy shows that the field has no influence on the morphology of dendritic arrays. The field does, however, cause severe distortion in the cellular array morphology. Cellular arrayed growth with the magnetic field results in an extensive channel formation in the mushy zone, as opposed to the well-aligned and uniformly distributed cells formed in the absence of the field. The channels are produced due to the anisotropy in the thermosolutal convection caused by the magnetic field. Macrosegregation, however, along the length of the directionally solidified samples is not influenced by this magnetic field for either the cellular or dendritic arrays.

I. INTRODUCTION

DIRECTIONAL solidification of binary alloys in a positive thermal gradient, with melt on the top, solid below, and gravity pointing down, may produce a solutal profile in the interdendritic mushy region and in the melt immediately ahead of the cellular/dendritic array, which promotes thermosolutal convection. A systematic investigation of macrosegregation resulting from such thermosolutal convection in Pb-Sn alloys has recently been reported.[1,2] Unlike Al-Cu alloys, which produce dendrite steepling when directionally solidified at low gradients of constitutional supercooling,[3,4] the array morphology is observed to be uniform across the sample cross section in Pb-Sn alloys.[5] This makes it possible to measure the tip radii, especially of cells, by successively polishing longitudinal sections near quenched array tips for a quantitative comparison with theoretical models. However, theoretical models for constrained growth of cellular/dendritic arrays assume purely diffusive transport and do not include convection. The purpose of this study was to explore the possibility of using magnetic field to suppress the thermosolutal convection which is present during steady-state directional solidification of cellular/dendritic arrays in Pb-Sn alloys.

The application of a magnetic field to suppress convection during directional solidification has been investigated, especially for electronic materials.[6,7,8] These studies, concerned mostly with planar liquid-solid interface, have shown that convective flows in the melt can be significantly reduced by application of magnetic fields. However, for constrained growth of cellular/dendritic arrays during directional solidification, the influence of an applied magnetic field has not been studied. Boettinger *et al.*[9] examined the influence of transverse and axial magnetic fields in off-eutectic Pb-57 wt pct Sn alloy for growth conditions expected to produce a planar liquid-solid interface with an aligned two-phase composite microstructure. The microstructures of these alloys, however, contained only a small volume fraction of primary dendrites. Application of a magnetic field (0.1 T, transverse to the growth direction) had no influence on the microstructure or longitudinal macrosegregation. In this article, we examine the influence of a stronger transverse magnetic field (0.45 T) on the microstructure and macrosegregation during steady-state cellular/dendritic arrayed growth of Pb-Sn alloys.

Two growth conditions, (1) where convection is due to the density profile of the interdendritic melt and (2) where convection results from the solutal buildup in the melt ahead of the array tips, have been examined by selecting suitable alloy composition and growth speeds. In an earlier study[1] on directionally solidified hypoeutectic Pb-Sn alloys, a maximum in the longitudinal macrosegregation was observed for Pb-33.3 wt pct Sn. This indicated extensive thermosolutal convection in the interdendritic melt. Therefore, alloys with similar composition, Pb-38.7 wt pct Sn, were selected for examining the effect of a magnetic field on the thermosolutal convection. The longitudinal macrosegregation in Pb-17 wt pct Sn was observed to be minimal,[1] indicating minimal convection of the interdendritic liquid. In this study, therefore, alloys with similar tin content, but grown at much smaller growth speeds, have been used to investigate the influence of a magnetic field on the convection caused by the solute buildup in the bulk melt at the array tips.

II. EXPERIMENTAL PROCEDURE

Precast Pb-Sn alloy samples (about 30-cm long) contained in quartz crucibles (0.7-cm ID) were remelted (melt column about 20-cm long) in vacuum and directionally solidified in a modified Bridgman apparatus by raising the furnace assembly at various speeds with respect to the stationary crucibles, thus avoiding convection possibly caused by the crucible motion. Growth conditions were thermally stable, with the melt on top and the solid below, with gravity pointing down. The directional solidification furnace was equipped with a 0.5 T electromagnet with a pole diameter of 15 cm and a pole separation of 15 cm. Samples were directionally solidified with and without the 0.45 T magnetic field, applied

S.N. TEWARI, Professor, and HUI SONG, Research Associate, are with the Chemical Engineering Department, Cleveland State University, Cleveland, OH 44115. RAJESH SHAH, formerly Graduate Student, Chemical Engineering Department, Cleveland State University, is with Agmet Metals Inc., Oakwood Village, OH 44146.

Manuscript submitted February 25, 1993.

transverse to the growth direction, with otherwise identical growth conditions. After 10 to 12 cm of directional growth, the samples were quenched by directing a jet of helium gas, cooled by liquid nitrogen, onto the surface of the quartz crucibles. The furnace and crucible arrangements are such that for the growth conditions studied, the furnace translation speed is equal to the directional solidification speed. This was ascertained by correlating the longitudinal microstructure of directionally solidified samples with the furnace translation distance. As shown in Figure 1, the mushy zone length in these experiments was much smaller than the length of the initial melt column. A steady-state thermal profile was maintained at the liquid-solid interface,[5] thus ensuring a nearly constant mushy zone length during entire directional solidification.

Figure 1 shows a typical thermal profile within the sample during directional solidification of Pb-23.2 wt pct Sn grown at 6 μm s^{-1}. Also shown is the profile of the magnetic field strength measured at room temperature along the axis of an empty crucible and a schematic view of a solidifying sample. In this figure, the locations of the mushy zone at the start of solidification, $H_{initial}$, and at the end of solidification (at the time of quench), H_{final}, are also shown.

The longitudinal (parallel to growth direction) and transverse microstructures were examined in the unetched condition by optical metallography. Several transverse sections in the quenched mushy zone, at varying distance from the dendrite tips, were examined. The samples themselves did not provide adequate gray level contrast for electronic image analysis. The cell boundaries, therefore, were traced by hand from montages which were made up of many transverse micrographs. These tracings were used to determine the cellular size distributions by making use of the image analysis software, JAVA.[10] The perimeter of each cell was measured and the cell size was assumed to be equal to the diameter of a circle with the same perimeter. The number of sides on the cells was also measured.

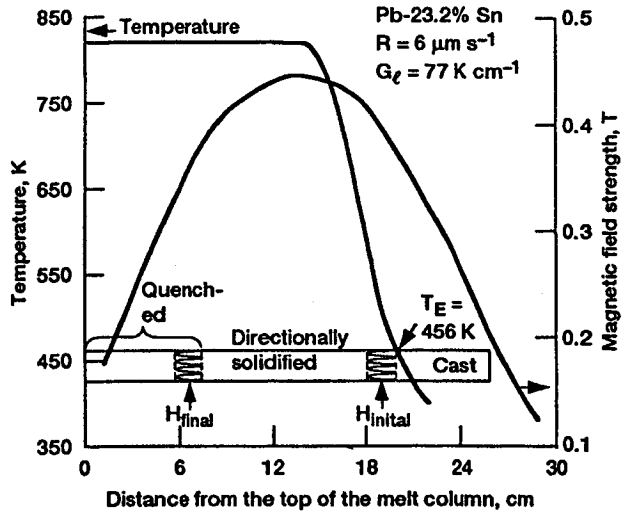

Fig. 1—Typical thermal and magnetic field intensity profile during directional solidification of a Pb-Sn alloy. This figure also shows a schematic view of a typical sample being directionally solidified, with the initial and final locations of the mushy zone.

Atomic absorption spectrometry was used to analyze the tin content along the length of the directionally solidified bars. The tin contents of the thin slices (~3-mm wide), cut along the length, were determined to an accuracy of ±5 pct. Distance from the tip of the mushy zone at the onset of directional solidification to its tip at the time of quench is taken as the total distance solidified. The ratio of the distance solidified to the total length of the initial melt column is taken as the fraction solid (f_s). Electron microprobe analyses were used in an area scan mode (40 × 40 μm) to obtain the radial macrosegregation on sections transverse to the growth direction.

III. RESULTS

As mentioned earlier, a steady-state thermal profile was maintained throughout solidification; however, the magnetic field did not remain constant. For example, for the sample shown in Figure 1, the magnetic field strength at the array tips was about 0.41 T at the start of solidification, achieved a maximum of 0.45 T, and dropped to about 0.32 T just before quench.

IV. MICROSTRUCTURE

Figures 2 through 5 show typical longitudinal (at the quenched liquid-solid interface) and transverse (in the quenched mushy zone at some distance from the tip) microstructures of samples solidified with and without the application of the magnetic field. The behaviors of the samples solidified with dendritic microstructures are indicated in Figures 2 and 3, and those solidified with cellular microstructures are represented in Figures 4 and 5. As described later, the application of the magnetic field had no discernible influence on the dendritically grown samples. However, its application significantly affected the mushy zone morphology of the cellular samples.

A. *Dendritic Array*

Figure 2 shows the microstructure of a Pb-33.3 wt pct alloy, which was grown at 8 μm s^{-1}, and a temperature gradient in the liquid (G_l) of 75 K cm^{-1}. Figure 2(a) shows the well-aligned array of primary dendrites. The uniform distribution of primary dendrites is indicated by Figure 2(b). The dendrites are uniformly distributed across the entire sample cross section, as seen in Figure 2(c), except for the two channels located on the surface. As described in a previous publication,[1] the channels, when present, were invariably located on the surface of the dendritically grown samples.

Figure 3 shows the microstructure of a Pb-38.7 wt pct Sn alloy directionally solidified with an applied magnetic field. Growth conditions for this sample were otherwise identical to the sample shown in Figure 2. Comparison of Figures 2 and 3 shows that the application of the magnetic field had no influence on the microstructure of dendritically grown samples. Distribution of the primary dendrites is uniform across the cross section (Figures 3(a) and (b)), similar to the sample grown without the magnetic field (Figures 2(b) and (c)). The sample

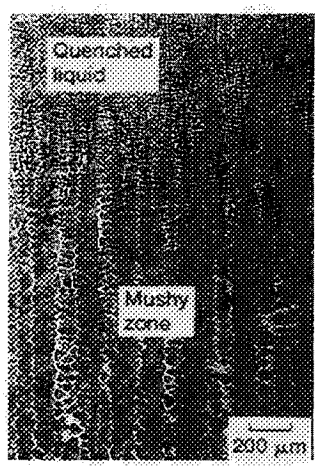

(*a*) **Longitudinal (parallel to the growth direction at quenched liquid-solid interface).**

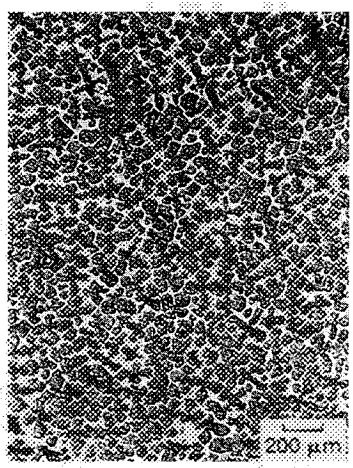

(*b*) **Transverse (below the eutectic isotherm).**

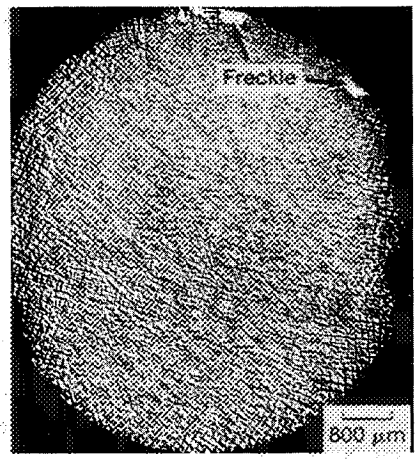

(*c*) **Overall transverse view of the sample. Freckles are marked by arrow.**

Fig. 2—Dendritic microstructure of Pb-33.3 wt pct Sn (G_l = 75 K cm^{-1}, R = 8μm s^{-1}) solidified without the magnetic field. (*a*) Longitudinal (parallel to the growth direction at quenched liquid-solid interface). (*b*) transverse (below the eutectic isotherm). (*c*) overall transverse view of the sample. The freckles are marked by an arrow.

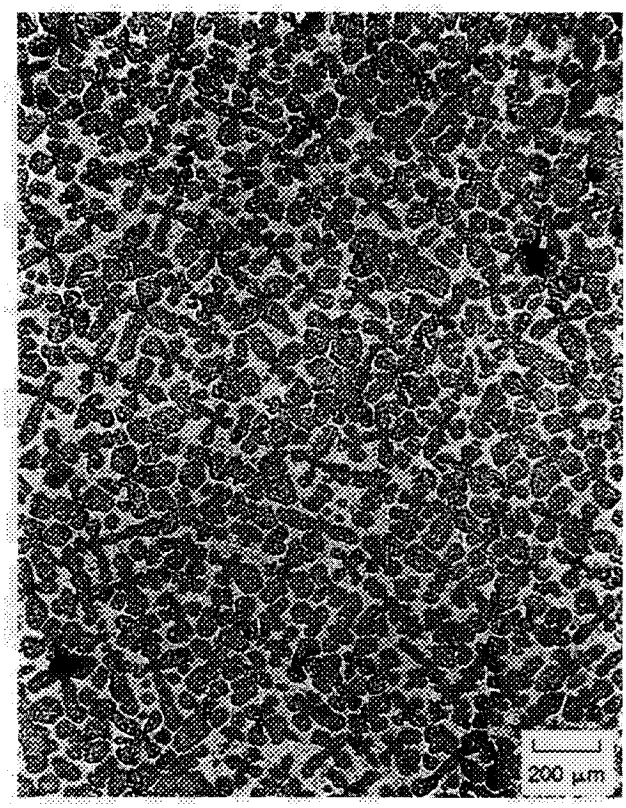

(*a*) **Transverse (below the eutectic isotherm).**

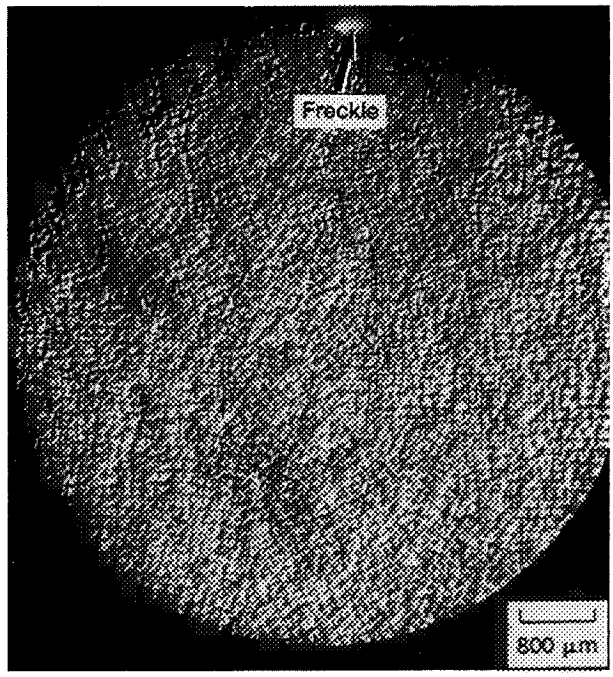

(*b*) **Overall transverse view of the sample. Freckle is marked by arrow.**

Fig. 3—Dendritic microstructure of Pb-38.7 wt pct Sn (G_l = 75 K cm^{-1}, R = 8 μm s^{-1}) solidified with a 0.45 T transverse magnetic field. (*a*) Transverse (below the eutectic isotherm). (*b*) overall transverse view of the sample. The freckle is marked by an arrow.

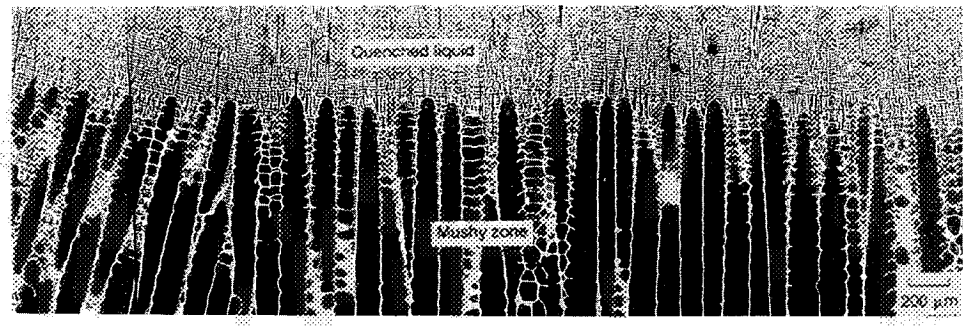

(*a*) Longitudinal (near quenched tips).

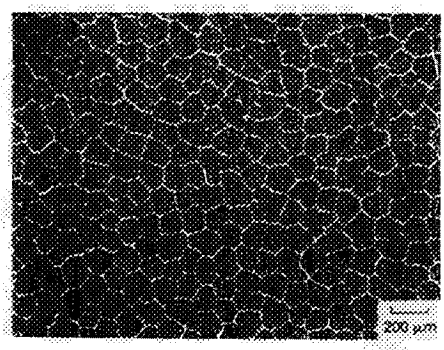

(*b*) Transverse (6.5 mm from the tips in the quenched mushy zone).

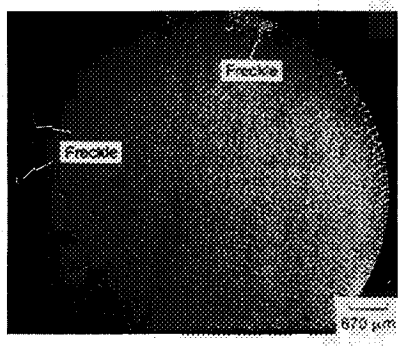

(*c*) Overall transverse view (6.5 mm from the tips in the quenched mushy zone). Freckles are marked by arrows.

Fig. 4—Cellular (near cell to dendrite transition) microstructures of Pb-17.7 wt pct Sn (G_l = 101 K cm^{-1}, R = 1.0 μm s^{-1}) solidified without the magnetic field. (*a*) Longitudinal (near-quenched tips). (*b*) transverse (6.5 mm from the tips in the quenched mushy zone). (*c*) overall transverse view (6.5 mm from the tips in the quenched mushy zone). The freckles are marked by arrows.

grown with the magnetic field also had a channel located at the outer surface.

B. *Cellular Array*

Microstructures of Pb-17 wt pct Sn alloys are shown in Figure 4. At 4 μm s^{-1}, the microstructure (not shown in Figure 4) was dendritic, similar to Figure 2 for the Pb-33.3 wt pct Sn alloy, but with a much smaller interdendritic fraction of eutectic. At the lower growth speed of 1 μm s^{-1}, the microstructure was cellular (near cell to dendrite transition), and at 0.35 μm s^{-1}, it was perfectly cellular. Figure 4(a) shows the typical cellular array morphology for the Pb-17.7 wt pct Sn alloy grown at 1 μm s^{-1}, with a thermal gradient in the liquid of 101 K cm^{-1}. The cells are uniformly distributed across the entire sample cross section. This is observed more clearly at a lower magnification (Figure 4(c)). This sample also has three freckles. The cellular samples grown at slower growth speeds tended to have more freckles, again located mostly on the surface of the samples. Unlike the dendritically grown samples, the microstructures of the samples with cellular morphology are severely affected by the magnetic field (compare Figure 5 to Figure 4). Application of the magnetic field resulted in a nonuniform mushy zone. Tin-rich regions dispersed throughout the quenched mushy zone were observed (Figure 5(a)). Comparison of microstructure in these tin-rich regions in the mushy zone with the quenched melt ahead of the cell tips (Figure 5(a)) suggests that these regions consisted of pockets of liquid during directional solidification. This microstructure is very different from the well-aligned and uniformly distributed cells observed along the entire sample cross section in samples solidified with identical growth conditions, but without the magnetic field (Figure 4(a)). The transverse microstructure consists of islands of uniformly distributed cells (marked *A* in Figures 5(b) and (c)) separated by tin-rich channels (marked *B* in Figures 5(b) and (c)). In addition, there are several tin-rich nearly circular features (marked *C* in Figures 5(b) and (c)). The lower magnification view shown in Figure 5(c) provides a better representation of the overall microstructure. The tin-rich channels (*B* features) are aligned nearly normal to the magnetic field direction (the transverse magnetic field direction is marked by $\vec{B}$ in Figures 5(b) and (c)). The circular features *C* are invariably connected to the channels *B*.

Figure 5(d) shows a three-dimensional (3-D) sketch of the circular feature *C* and the major channel *B*, which is associated with it. Ten different transverse sections (*A* through *J*) in the mushy zone were superimposed to obtain this sketch. Section *A* was at 0.47 cm from the array tip and section *J* was at 0.05 cm. The *Z* axis is parallel to the alloy growth direction, and the *X-Y* plane is the plane of transverse section. The dark helix is the 3-D sketch of the circular feature *C* in Figure 5(c). The dotted lines in Figure 5(d) do not have any physical significance and are included only to ease the visualization of the helical nature of *C*. The helix, however, does not have a uniform pitch. The solid lines, connected to the

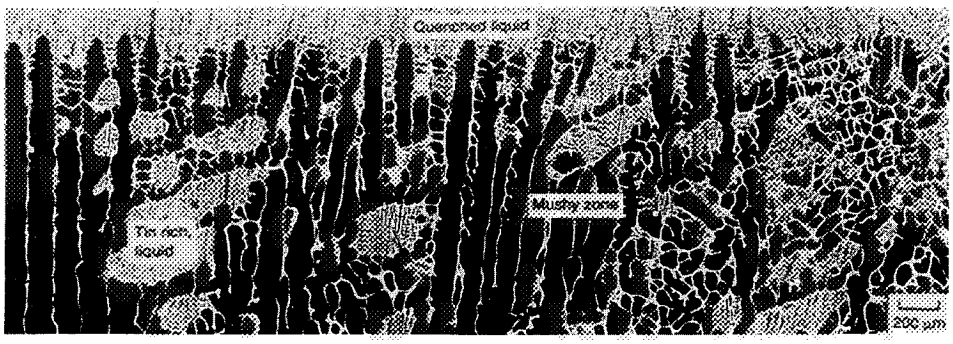

(*a*) Longitudinal (near Quenched tips).

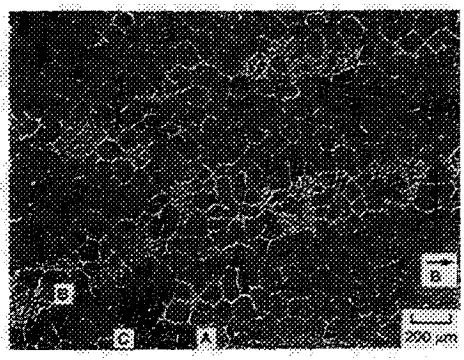

(*b*) Transverse (6.7 mm from the tips in the quenched mushy zone).

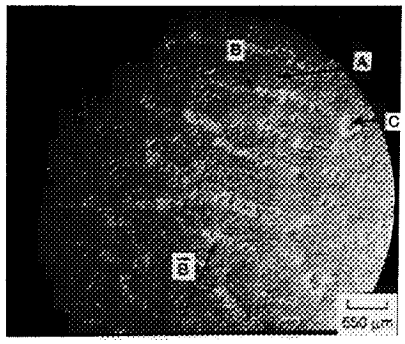

(*c*) Overall transverse view (6.7 mm from the tips in the quenched mushy zone).

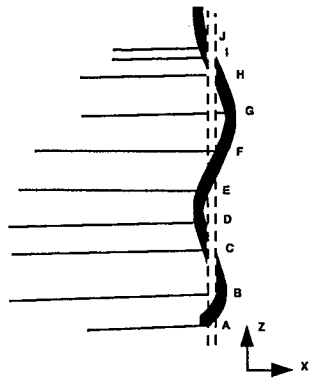

(*d*) Three dimensional visualization of circular features 'C' in Fig (c) and its associated major channel "B".

Fig. 5—Influence of magnetic field on cellular microstructures of Pb-18.2 wt pct Sn (G_l = 101 K cm^{-1}, R = 1.0 μm s^{-1}). Direction of the magnetic field is indicated by $\vec{B}$. (*a*) Longitudinal (near-quenched tips). (*b*) Transverse (6.7 mm from the tips in the quenched mushy zone). (*c*) Overall transverse view (6.7 mm from the tips in the quenched mushy zone). (*d*) 3-D visualization of circular features C in Fig. (c) and its associated major channel B.

helix at the 10 transverse sections, represent the major tributary that culminated into the helix (feature *B* in Figure 5(c)). When viewed on the transverse plane (plane *X-Y*), the helical feature did not appear to change its location significantly along the mushy zone length. However, the feature *B*, aligned nearly normal to the applied magnetic field, showed significant variation along the mushy zone length. As will be seen later, these helical features (*C*) are caused by the upward localized flow (plumes) of the tin-rich melt in the vicinity of the cell tips. The upward plumes are fed by the intercellular melt flowing through the river-like channels (*B*) in the mushy zone.

V. LONGITUDINAL MACROSEGREGATION

In this section, we examine the influence of the magnetic field on the longitudinal macrosegregation produced with the two growth conditions: (1) where convection is due to the density profile of the interdendritic melt and (2) where convection is mainly due to the solute buildup in the melt ahead of the array tips. Radial thermal gradients are quite small during growth of these samples, as indicated by the constant mushy zone height seen in the longitudinal sections. The influence of an applied magnetic field on the longitudinal macrosegregation for these two growth conditions is shown in

Figures 6 and 7. These figures plot C_s/C_o *vs* fraction solidified (f_s). The open symbols correspond to the samples solidified without the magnetic field, and the closed symbols correspond to those with the 0.45 T magnetic field. Extensive longitudinal macrosegregation along the length of the directionally solidified sample is interpreted as evidence of convection. In the absence of convection, most of the sample length (except for an initial small length about the length of the mushy zone) would be expected to have the original solute content, *i.e.*, $C_s/C_o=1$.

For the Pb-38 wt pct Sn alloy, growing at 8 μm s^{-1} and G_l = 75.4 K cm^{-1}, very little tin buildup in the melt ahead of the dendritic array is expected. $[C_t - C_o]/C_o$ is estimated to be about 0.02 from an analytical model of dendrites, which does not include convection in its analysis,[11] where C_t is tin content of the melt at the array tip and C_o is that of the alloy. The convection responsible for the longitudinal macrosegregation (Figure 6) is therefore mainly due to the interdendritic solutal gradients.[1] Figure 6 shows that the magnetic field has no influence on the intensity of longitudinal macrosegregation for dendritic samples grown with conditions where interdendritic thermosolutal convection is dominant; the macrosegregation profiles are almost identical for the samples grown with and without the field.

The influence of the magnetic field on the convection due to the solutal buildup in the melt ahead of the cellular/dendritic array is shown in Figure 7 for the Pb-18 wt pct Sn alloy grown at G_l = 101 K cm^{-1}. Decreasing the growth speed results in more macrosegregation, as shown in Figure 7(a). In this figure, the multiple data at a fraction solid denote the transverse macrosegregation. These compositions were obtained by machining the sample in a lathe and analyzing the chips. The high values of C_s/C_o in the very beginning of solidification are probably due

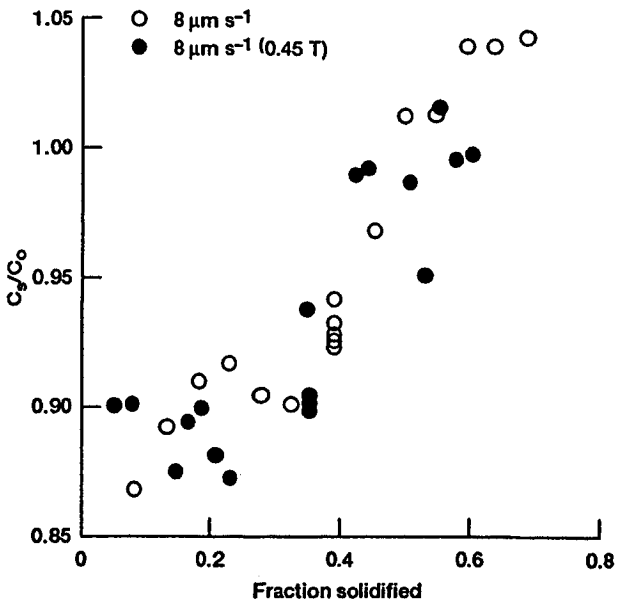

Fig. 6—Longitudinal macrosegregation for dendritic samples grown with and without the application of a transverse magnetic field (G_l = 75 K cm^{-1}, R = 8 μm s^{-1}; filled symbols are for Pb-38.7 wt pct Sn grown with a magnetic field, and open symbols are for Pb-33.3 wt pct Sn grown without the magnetic field).

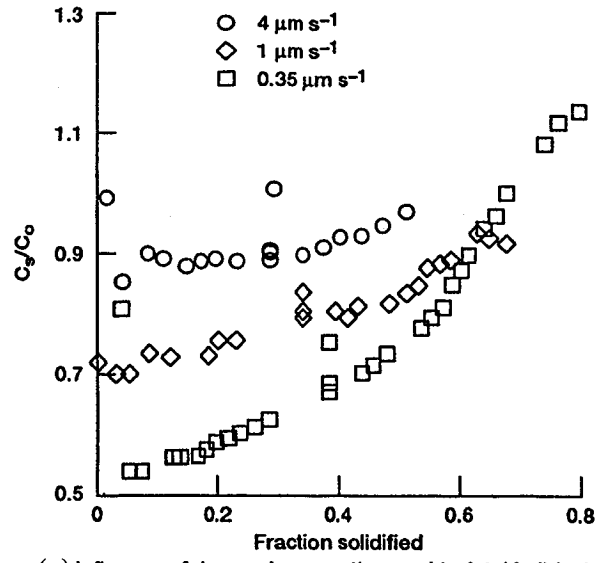

(*a*) Influence of decreasing growth speed (solutal buildup).

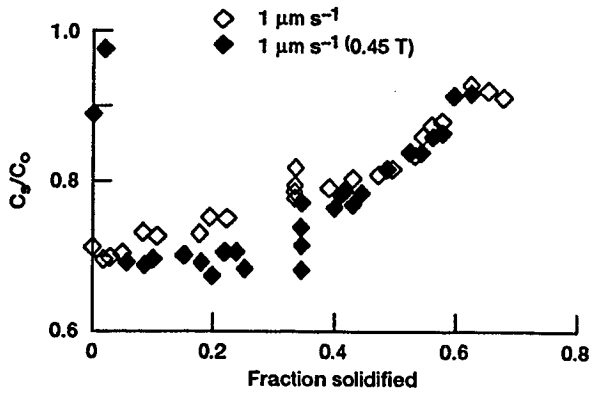

(*b*) Influence of magnetic field R = 1.0 μm s^{-1}.

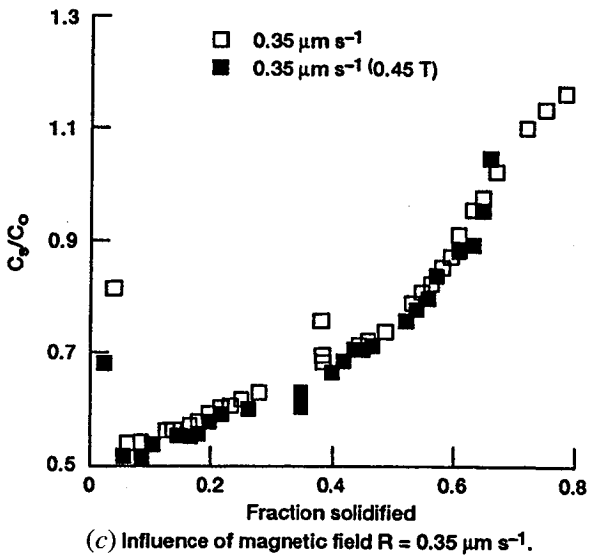

(*c*) Influence of magnetic field R = 0.35 μm s^{-1}.

Fig. 7—Longitudinal macrosegregation caused by convection due to solutal buildup at the array tips and influence of magnetic field (filled symbols are for samples grown with the magnetic field, and open symbols are for those grown without). (*a*) Influence of decreasing growth speed (solutal buildup). (*b*) Influence of magnetic field, R = 1.0 μm s^{-1}. (*c*) Influence of magnetic field, R = 0.35 μm s^{-1}.

to the shrinkage driven inverse segregation effect and will not be discussed here. As described previously[2] for the cellular morphologies, the decreasing growth speed is expected to result in an increased solutal buildup ahead of the array (in this alloy, $[C_l - C_o]/C_o$ is estimated to be 0.2, 0.5, and 1, respectively, for growth speeds of 4, 1, and 0.35 μm s^{-1}). The convection is more intense and results in more longitudinal macrosegregation. The magnetic field, despite its large influence on the morphology of the mushy zone for cellular arrays (Figure 5), has no influence on the extent of longitudinal macrosegregation (Figures 7(b) and (c)). The macrosegregation profiles are virtually identical for samples grown with and without the magnetic field for both the samples solidified at 1 μm s^{-1} (Figure 7(b)) and at 0.35 μm s^{-1} (Figure 7(c)).

VI. DISCUSSION

During directional solidification of hypoeutectic Pb-Sn alloys, a positive thermal gradient creates a stabilizing density gradient in the melt (density decreasing with height, with gravity pointing down). However, as schematically shown in Figure 8(a), the solutal profile creates a destabilizing density gradient, with density increasing with height. The solute buildup ahead of the dendrite array decreases over a distance approximately equal to D_l/R, where D_l is the solute diffusivity in the melt and R is the growth speed. Therefore, the melt density increases to ρ_{max} before the influence of the positive thermal gradient causes the density to decrease. Such a density profile leads to convective instability at the array tips.[2]

Convective mixing between the interdendritic and the overlying melt during growth is responsible for the experimentally observed macrosegregation along the length of the directionally solidified samples. Despite the extensive longitudinal macrosegregation, the distribution of primary dendrites (Figure 2) and cells (Figure 3) is uniform across most of the cross section in the samples grown without the magnetic field. This observation suggests that in the absence of magnetic field, convection must be through many small cells which are uniformly distributed across the liquid-solid interface, except near the crucible walls, where freckles were observed. This is in agreement with a recent suggestion[13] that uniformly distributed convection cells, with hexagonal appearance on the specimen cross section, are formed ahead of the mushy region due to porosity fluctuations in the mushy zone. The fluid flows upward at the edges of the hexagons and downward in their interior. The upward flow is strongest at the nodes of the hexagons and may lead to the formation of "chimneys" (plumes) at these locations. This is also in agreement with a recent numerical examination of the instabilities by Worster.[14] He predicted two types of instabilities: one ("boundary-layer mode"), driven by the solutal buildup ahead of the array, has a wavelength of the order of the solute boundary layer thickness; and the other ("mushy-layer mode") has a wavelength of the order of the mushy zone length. The convection cells due to the boundary-layer mode correspond to those described by Tait *et al.*[13] These would be localized in the vicinity of array tips and would be uniformly distributed across the specimen cross section.

Any anisotropy in the fluid flow would be expected to intensify some of these convection cells at the expense of others, ultimately leading to the formation of channels of solute-rich (low-density) plumes emerging from the mushy zone into the overlying melt, as has been observed in transparent organic analogues.[15] As shown recently by a numerical analysis,[16] any anisotropy in the fluid flow leads to a localized accumulation of solute. For example, the horizontal component of the fluid velocity is zero at the mold walls because of the no-slip condition. During convection, the moving fluid is always in local thermal equilibrium with the melt because of the high thermal diffusivity of the melt, 1.1×10^{-5} m^2 s^{-1}.[15] However, because of the low solutal diffusivity, 3×10^{-9} m^2 s^{-1},[15] the solute being carried in the convecting stream is not allowed to mix with the rest of the melt. This causes an increase in the solute content in the melt in the vicinity of the mold walls, resulting in localized regions of reduced density. These regions lead to the formation of channels (Figures 3 and 4) in which tin-rich (low density) plumes rise upward. The channels are fed and sustained by interdendritic fluid flow in the mushy zone. The intensity of convection increases with decreasing growth speed because of the higher solutal buildup and increased density inversion ahead of the array. Hence, the cellular arrays have a higher probability of forming these channel segregates than the dendritic arrays because they are grown at slower rates. This was observed in the present work.

A. *Influence of Transverse Magnetic Field*

Motion of the electrically conducting melt in the presence of an applied magnetic field causes an electric current ($\vec{J}$) to flow in a direction normal to the fluid velocity ($\vec{V}$) and applied magnetic field ($\vec{B}$). This current in the presence of the magnetic field leads to a force ($\vec{J} \times \vec{B}$) opposing the motion (the Lorentz force). This force is sometimes considered as an added effective fluid viscosity for qualitative purposes. Effectiveness of the magnetic field in damping convective flows depends on the value of the Hartman number[6] ($\mu\beta L\sqrt{(\sigma/\eta)}$, where β is magnetic field strength (0.45 T), σ is electrical conductivity (3.1×10^6 Ω^{-1} m^{-1}[17]), η is viscosity (2×10^{-3} N s m^{-2}[17,18]), μ is relative magnetic permeability (1[19]) and L is a characteristic length of the system. Because the magnetic field is transverse to the alloy growth direction, the inside diameter of the crucible, 0.7 cm, can be taken as the characteristic length. The Hartman number for our growth conditions is 124. This value is much larger than the Hartman number of 54 observed to dampen the convection completely by application of a vertical magnetic field during Czochralski growth of molten gallium.[20] It suggests that application of the magnetic field during our experiments significantly reduced the fluid velocities normal to the field. However, flow parallel to the applied field ($\vec{B}$) is not effected by the field.

Lehnert and Little[21] examined the convection pattern on the surface of a mercury melt that was heated from

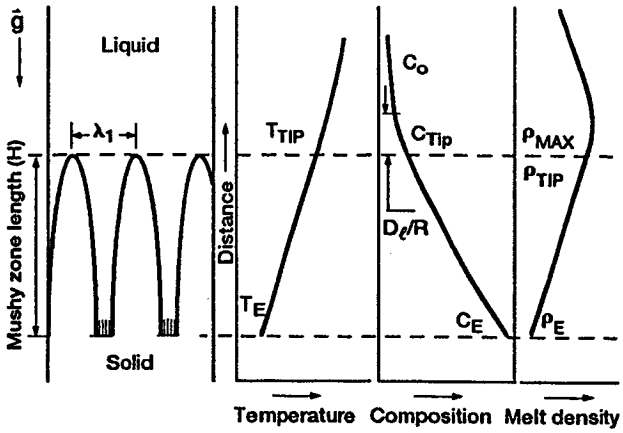

(*a*) **Schematic presentation of melt density during directional solidification of Pb-10 wt pct Sn alloy in a positive thermal gradient of 110 K cm^{-1} at 2 μm s^{-1}.**

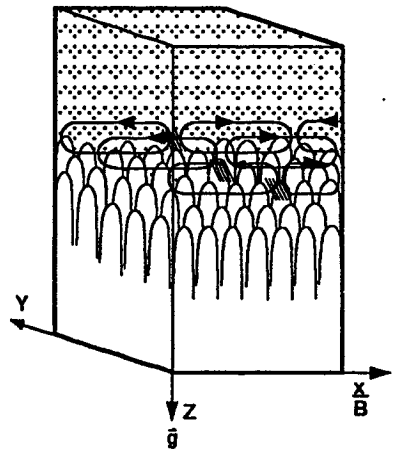

(*b*) **Anisotroby in the fluid flow introduced by the applied magnetic field (B) results in convection rolls which are elongated in the direction of the magnetic field and lie on the plan containing the magnetic field (B) and the gravity vector (g). The magnetic field significantly reduces the fluid velocity normal to the field, and leads to solute accumulation indicated by the hatched regions.**

Fig. 8—Influence of magnetic field on the nature of convection adjacent to the cellular array tips. (*a*) Schematic presentation of melt density during directional solidification of a hypoeutectic Pb-Sn alloy in a positive thermal gradient. (*b*) Anisotropy in the fluid flow introduced by the applied magnetic field ($\vec{B}$) results in convection rolls which are elongated in the direction of the magnetic field and lie on the plane containing the magnetic field ($\vec{B}$) and the gravity vector (g). The magnetic field significantly reduces the fluid velocity normal to the field and leads to solute accumulation indicated by the hatched regions.

below. At the onset of instability, they observed uniformly distributed cells across the melt surface. However, application of a transverse magnetic field caused the convection cells to elongate in the direction of the magnetic field, in agreement with the predictions by Chandrasekhar.[22] Chandrasekhar predicted that in the presence of a transverse magnetic field, the cells, which appear at the onset of instability, must be longitudinal rolls in directions parallel to the plane containing the magnetic field, ($\vec{B}$), and g. He also predicted that only the component of magnetic field, which was oriented parallel to the gravity, would be effective in suppressing the onset of thermal convection. In the absence of similar studies applied to thermosolutal convection, we assume that the effects of transverse magnetic field on the convection cells during our experiments are similar to that observed for the thermal instability. We expect, therefore, a behavior schematically indicated in Figure 8(b), which shows three typical convection rolls parallel to the plane containing ($\vec{B}$) and $\vec{g}$. Also, the fluid velocity normal to the magnetic field will be less than that parallel to ($\vec{B}$). Because of the low Lewis number, approximately 10^{-4}, a significant portion of the solute accumulated in the fluid stream, which was flowing parallel to the magnetic field near the array tips, will be left behind when the flow changes its direction, *i.e.*, the solute-rich fluid is forced to decelerate as it begins to rise because of the transverse magnetic field. This causes solute accumulation along a direction nearly normal to ($\vec{B}$), as indicated by the hatched regions in Figure 8(b). This may be responsible for the experimentally observed tin-rich regions in the mushy zone near the array tips, which are aligned nearly perpendicular to the applied magnetic field (marked $\vec{B}$ in Figure 5). Since the uniform distribution of small convection cells and fluid plumes can no longer be sustained in the presence of transverse magnetic field, large localized vertical channels also develop in the microstructure (marked as *C* in Figure 5). It is not clear, however, why these channels assume an approximately helical shape.

B. *Influence of Magnetic Field on Cell Distribution*

As seen above, the application of a transverse magnetic field (0.45 T) does not decrease the convection responsible for the longitudinal macrosegregation. In addition, it causes channel formation in the mushy zone, resulting in inhomogeneities in the cellular distributions. As opposed to the uniform distribution of the cells across the entire sample cross section (Figure 4) for growth without the applied magnetic field, the distribution is nonuniform in the samples grown with the magnetic field (Figure 5). An examination of Figures 5(b) and (c) shows that the nonuniformity is larger in the vicinity of the channels (region *B*) than in the island regions away from these channels (region *A*). The intercellular volume fraction is also higher in the channel vicinity than in the regions away from the channels (Figure 5(b)).

The influence of the magnetic field on the cellular distribution is more clearly evident in Figure 9, which presents histograms for the cell size (diameter of a circle with perimeter equal to that of the cell) and their coordination number (number of sides). Statistical analyses[23] of the data, using the *F* test to compare the "standard deviations" and the "Aspin Welch Test" for comparing the means, shows that growth under the magnetic field results in reduced cell size [154 ± 39 μm (Figure 9(a)) *vs* 122 ± 40 μm (Figure 9(b)); the two means are different at a confidence level of 99.5 pct]. Distribution of the cells is approximately hexagonal in nature. However, smaller mean coordination number and larger scatter are observed for the specimen grown under the magnetic field than for that grown without the field (5.59 ± 1.21 (Figure 9(d)) *vs* 5.76 ± 1.03 (Figure 9(c));

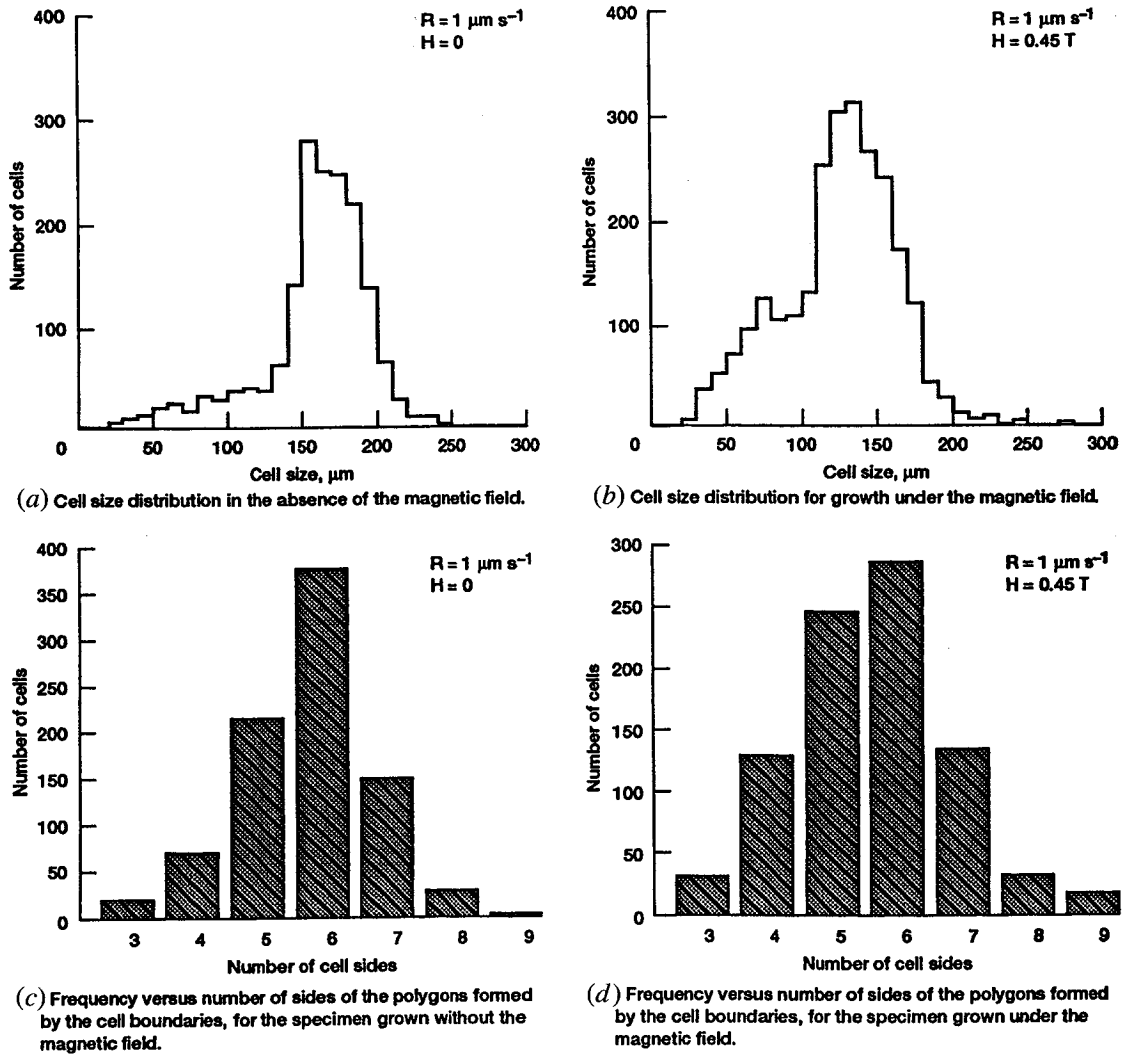

Fig. 9—Influence of magnetic field on the cell size and shape distribution, observed on the transverse section of the sample, for Pb-18 wt pct Sn (G_l = 101 K cm^{-1}). (*a*) Cell size distribution in the absence of the magnetic field. (*b*) Cell size distribution for growth under the magnetic field. (*c*) Frequency *vs* number of sides of the polygons formed by the cell boundaries, for the specimen grown without the magnetic field. (*d*) Frequency *vs* number of sides of the polygons formed by the cell boundaries, for the specimen grown under the magnetic field.

the two means and standard deviations are different at a confidence level of 99.5 pct). It is obvious that a 0.45 T transverse magnetic field cannot be used to suppress convection and grow cellular arrays suitable for comparison with theoretical models. There is a need to carry out similar studies in the presence of large axial magnetic fields, applied parallel to the alloy growth direction. If the convection still can not be suppressed, then the critical quantitative cell morphology data for determining the cellular shape selection criterion during constrained growth of binary alloys can only be obtained by partial directional solidification and quenching experiments carried out in the low gravity environment of space.[2,24]

VII. CONCLUSIONS

The following conclusions can be drawn from this study, where the effect of magnetic field (0.45 T), applied transverse to the growth direction in directionally solidified Pb-Sn alloys, has been examined on the macrosegregation and mushy zone morphology.

1. Directional solidification of hypoeutectic Pb-Sn alloys in a positive thermal gradient results in gravity-induced thermosolutal convection, both in the mushy zone and in the bulk melt ahead. This produces longitudinal (parallel to the alloy growth direction) macrosegregation.
2. The extent of the longitudinal macrosegregation is greater for the cellular arrays than for the dendritic arrays. The transverse magnetic field has no influence on the extent of the bulk convective mixing, as indicated by the longitudinal macrosegregation, which is identical for the samples grown with and without the magnetic field. This observation is valid for both the cellular and the dendritic arrays.
3. Application of a transverse magnetic (0.45 T) field does not influence the morphology of dendritic arrays. However, the anisotropy in the fluid flow introduced by the field has a strong influence on the

morphology of cellular arrays. It causes channel formation in the mushy zone and nonuniformity in the cell size distribution.

ACKNOWLEDGMENTS

Support for this research from the Microgravity Materials Science Laboratory at the NASA-Lewis Research Center, Cleveland, OH, and from the NASA-Microgravity Science and Applications Division is gratefully acknowledged. Appreciation is expressed to Thomas K. Glasgow for helpful discussions, to David H. Matthiesen for careful review, and to David A. Thompson for help in the 3-D visualization of the channels.

REFERENCES

1. S.N. Tewari and R. Shah: *Metall. Trans. A*, 1992, vol. 23A, pp. 3383-92.
2. S.N. Tewari, R. Shah, and M.A. Chopra: *Metall. Trans. A*, 1993, vol. 24A, pp. 1661-69.
3. M.H. Burden, D.J. Hebditch, and J.D. Hunt: *J. Cryst. Growth*, 1973, vol. 20, pp. 121-24.
4. M.D. Dupouy, D. Camel, and J.J. Favier: *Acta Metall.*, 1989, vol. 37, pp. 1143-57.
5. M.A. Chopra and S.N. Tewari: *Metall. Trans. A*, 1991, vol. 22A, pp. 2467-74.
6. J.R. Carruthers: *Preparation and Properties of Solid State Materials—Vol. 3*, W.R. Wilcox and R.A. Lefever, eds., Marcel Dekker, Inc., New York, NY, 1977, pp. 1-113.
7. D.H. Matthiessen, M.J. Wargo, S. Motakef, D.J. Carlson, J.S. Nakos, and A.F. Witt: *J. Cryst. Growth*, 1987, vol. 85, pp. 557-60.
8. G.D. Robertson, Jr. and D.J. O'Connor: *J. Cryst. Growth*, 1986, vol. 76, pp. 100-10.
9. W.J. Boettinger, F.S. Biancaniello, and S.R. Coriell: *Metall. Trans. A*, 1981, vol. 12A, pp. 321-27.
10. "JAVA," from Jandell Scientific Corporation. (Our use of the "JAVA" image processing program does not necessarily endorse the use of this product).
11. V. Laxmanan: *J. Cryst. Growth*, 1986, vol. 75, pp. 573-80.
12. T.D. McCay, M.H. McCay, S.A. Lowry, and L.M. Smith: *J. Thermophys. Heat Transfer*, 1989, vol. 3 (3), pp. 345-50.
13. S. Tait, K. Jahrling, and C. Jaupart: *Nature*, 1992, vol. 359, pp. 406-08.
14. M. Grae Worster: *J. Fluid Mech.*, 1992, vol. 237, pp. 649-69.
15. A.K. Sample and A. Hellawell: *Metall. Trans. A*, 1984, vol. 15A, pp. 2163-73.
16. S.D. Felicelli, J.C. Heinrich, and D.R. Poirier: *Metall. Trans. B*, 1991, vol. 22B, pp. 847-59.
17. *Liquid Metals*, S.Z. Beer, ed., Marcel Dekker, Inc., New York, NY, 1972, p. 144.
18. Y.S. Touloukian, S.C. Saxena, and P. Hestermans: *Viscosity, Thermophysical Properties of Matter*, Plenum Publishing, New York, NY, 1975, vol. 11, p. 578.
19. *Metals Handbook*, ASM, Metals Park, OH, 1961, vol. 1, p. 1064.
20. G. Szabo, Z. Juhaz, J. Paitz, and J. Poltl: *J. Cryst. Growth*, 1986, vol. 78, pp. 558-60.
21. B. Lehnert and N.C. Little: *Tellus*, 1957, vol. 9, pp. 97-103.
22. S. Chandrasekhar: *Hydrodynamic and Hydromagnetic Stability*, Dover Publications, Inc., New York, NY, 1961, p. 92.
23. A.J. Duncan: *Quality Control and Industrial Statistics*, 4th ed., Erwin Publishers, Homewood, IL, 1974.
24. S.N. Tewari and R. Trivedi: *Microgravity Sci. Techno.*, 1991, vol. 4, pp. 191-99.